

A comparison of CT- and MR-based attenuation correction in neurological PET

John C. Dickson · Celia O'Meara · Anna Barnes

Received: 28 June 2013 / Accepted: 28 November 2013 / Published online: 15 January 2014
© Springer-Verlag Berlin Heidelberg 2013

Abstract

Purpose To assess the quantitative accuracy of current MR attenuation correction (AC) methods in neurological PET, in comparison to data derived using CT AC.

Methods This retrospective study included 25 patients who were referred for a neurological FDG PET examination and were imaged sequentially by PET/CT and simultaneous PET/MR. Differences between activity concentrations derived using Dixon and ultrashort echo time (UTE) MR-based AC and those derived from CT AC were compared using volume of interest and voxel-based approaches. The same comparisons were also made using PET data represented as SUV ratios (SUVr) using grey matter cerebellum as the reference region.

Results Extensive and statistically significant regional underestimations of activity concentrations were found with both Dixon AC ($P < 0.001$) and UTE AC ($P < 0.001$) in all brain regions when compared to CT AC. The greatest differences were found in the cortical grey matter (Dixon AC 21.3 %, UTE AC 15.7 %) and cerebellum (Dixon AC 19.8 %, UTE AC 17.3 %). The underestimation using UTE AC was significantly less than with Dixon AC ($P < 0.001$) in most regions. Voxel-based comparisons showed that all cortical grey matter and cerebellum uptake was underestimated with Dixon AC compared to CT AC. Using UTE AC the extent and significance of these differences were reduced. Inaccuracies in cerebellar activity concentrations led to a mixture of predominantly cortical underestimation and subcortical overestimation in SUVr PET data for both MR AC methodologies.

Conclusion MR-based AC results in significant underestimation of activity concentrations throughout the brain, which

makes the use of SUVr data difficult. These effects limit the quantitative accuracy of neurological PET/MR.

Keywords PET/MR · Attenuation correction · Quantification · Brain · PET

Introduction

The recent introduction of simultaneous PET/MR into the clinical imaging armoury is a significant development in medical imaging. There is much debate about the key roles and the potential of this new modality [1], but one role where there is significant potential is in the area of neuroimaging.

There is no doubt that the current imaging modality of choice in the brain is MRI. This is reflected in the clinic and in the literature with close to 20,000 publications recorded in PubMed in 2012 compared to 2,800 for CT, 1,100 for SPECT, and 2,600 for PET (using the keywords “Brain” with “MRI”, “CT”, “SPECT”, and “PET”, respectively). Nevertheless, although MR is able to measure function using techniques based on BOLD sequences and magnetic resonance spectroscopy, the ability of PET to measure function is superior to that of MRI both in sensitivity to signal, and in its direct measurement of physiological responses [2]. One thing that PET cannot offer, however, is high-resolution anatomical imaging. A combination of PET and MRI therefore offers great potential in the neuroimaging arena.

It has been argued that with automated image registration of PET and MR being widely available and easily applicable in the brain, simultaneous PET/MR is not necessary for neurological applications. However, the combined measurement of functional parameters on MR and PET is extremely attractive and is only possible with a simultaneous PET/MR instrument. Simultaneous acquisition also offers other opportunities such as the use of MR pulses or sequences to correct for

J. C. Dickson (✉) · C. O'Meara · A. Barnes
Institute of Nuclear Medicine, University College London Hospitals,
Euston Road, London NW1 2BU, UK
e-mail: john.dickson@uclh.nhs.uk

patient motion [3, 4], the ability to perform partial volume correction and *a priori* PET reconstructions [5–7], and the possibility of using gadolinium first-pass information to direct PET pharmacokinetics [8]. Furthermore, in neurooncology in which the utmost precision and same time-point imaging are required, simultaneous PET and MR would be preferable to a registration approach.

However, even with all these opportunities simultaneous PET/MR is not without its challenges. One of these challenges is using MR information for the accurate correction of PET photon attenuation. Unlike CT whose measurements of electron density can be directly translated into a reasonable attenuation map [9], MR typically provides a map of proton (hydrogen nuclei) density and relaxation properties of tissues, which cannot easily be converted into a form to correct for PET photon attenuation [10]. One of the current clinically available MR-based attenuation corrections (AC) is derived from the two-point Dixon gradient echo sequence [11]. By deriving information from echo times in which the signal from water and fat are in and out of phase, it is possible to create segmentation-based attenuation maps showing air (background), lungs, soft tissue (water) and fat [12]. Unfortunately, this method does not produce a bone signal, instead defining bone as soft tissue in attenuation maps. This has detrimental effects on PET image quality and accuracy, particularly in the brain which is surrounded by bone [13], and so Dixon based AC is not recommended for quantitative brain imaging [12].

Accepting the limitations of Dixon-based methods, equipment manufacturers and academic research groups have been working on improved solutions [14]. One such methodology which is being introduced into clinical use is based on an ultrashort echo time (UTE) sequence [15]. Bone typically has very short relaxation times, so the use of a UTE imaging sequence can capture bone information that can be incorporated into attenuation maps. Unfortunately, this is at the expense of an increased scan time. To our knowledge there are no investigations in the literature exploring the effect of current clinically available MR-based attenuation correction (MR AC) methods on patient data. The aim of this study is to do just this by comparing clinically available MR methods – namely the two-point Dixon-based approach (Dixon AC) and the UTE approach (UTE AC) – with a CT-based attenuation correction (CT AC).

In neuroimaging, in addition to providing PET information in terms of activity concentrations (or SUV), data can often be represented as SUV normalized to a reference region, which is known as SUV_r. Using data from FDG studies, this investigation compares CT AC and MR AC methods, with PET uptake defined in standard terms (activity concentrations), and also in terms of SUV_r referenced to a commonly used cerebellar reference region [16].

Materials and methods

Subjects

This retrospective study included 25 patients. The average age of the subjects was 37.1 years (range 23–62) with 12 men and 13 women. Of the 25 patients, 22 were referred to determine a possible epileptogenic focus, and 3 were referred to assess dementia. Based on clinical interpretation of the standard of care PET/CT scan, 18 of the 22 epileptic patients had abnormal areas of hypometabolism, and 2 of the 3 dementia patients had areas of hypometabolism. Approval for this study was given by the local ethics committee, with all patients giving informed consent for the data to be used in retrospective studies.

Image acquisition

FDG PET/CT data were acquired on GE Discovery ST and VCT PET/CT systems (GE Healthcare Systems, Waukesha, WI) and PET/MR data were acquired on a Siemens Biograph mMR system (Siemens Healthcare, Erlangen, Germany; software version VB18p). A summary of the acquisition parameters used is given in Table 1.

In 13 of the 25 patients PET/CT was performed before PET/MR at an average of 69.64 min (range 28–131 min) after injection. In the remaining 12 patients who had PET/MR first, the average time of imaging was 64.72 min (range 32–132 min) after injection. The difference in time after injection between the two groups was not significant ($p=0.59$) as determined using Student's *t* test. Furthermore, the uptake environment before the first scan, and transportation between the uptake area and the scanner were similar in the PET/CT and PET/MR suites.

To minimize potential misregistration of PET and attenuation correction data, patients were immobilized in the PET/CT scanner with a head restraint using straps, while in the PET/MR scanner the head position was severely restricted by the head coil and specifically designed minimally attenuating immobilization pads. Following image acquisition all PET/CT and PET/MR data were visually assessed to check the integrity of registration of the PET and AC data.

Image processing/analysis

Data preparation

We used the PET data acquired on the PET/CT scanner and reconstructed using CT AC as the gold standard. Comparisons between CT AC PET and data acquired on the PET/MR scanner and reconstructed using Dixon AC and UTE AC were assessed using both voxel and volume of interest (VOI) methodologies. The voxel-based analysis was chosen because of its

Table 1 Acquisition and reconstruction parameters used to create AC data on PET/CT and PET/MR scanners

Parameter	Scanner	
	GE discovery ST/VCT	Siemens Biograph mMR
PET		
Scan mode	3-D	3-D
Voxel size (mm)	1.95×1.95×3.27	1.40×1.40×2.03
Reconstruction	Three iterations, 20 subsets, 3-D Hanning filter (cut-off 4 mm)	Three iterations, 21 subsets, 3-D gaussian filter (3.5 mm FWHM)
Scan duration (min)	15	15
Attenuation correction	CT AC: 120 kVp, 300 mAs, pitch 1.75/1.375	Dixon AC: TE ₁ 1.23 ms, TE ₂ 2.46 ms, TR 3.6 ms, flip angle 10° UTE AC: TE ₁ 0.07 ms, TE ₂ 2.46 ms, TR 11.94 ms, flip angle 10°
Processing	CT AC reconstruction filter, multilinear conversion of HU to PET attenuation	Dixon AC: fat, water, air segmentation UTE AC: bone, water, air segmentation
Slice thickness (mm)	3.75	Dixon AC: 3.12 UTE AC: 1.6
Scan duration (min:s)	0:12	Dixon AC: 0:19 UTE AC: 1:40

ability to assess differences without bias to selected areas of interest, and the VOI approach is relatively commonly applied in quantitative neurological PET.

The first step in the analysis was to put all AC PET data into the same anatomical space. Using SPM8 (Statistical Parametric Mapping; Wellcome Institute, UCL, London, UK), the PET studies were registered to the PET template within SPM using a bounding box of (−88 −116 −80; 88 80 100) to ensure that the full cerebellum was included. The spatial normalization algorithm uses a 3-D nonrigid transformation model for warping a brain scan to a template. These nonrigid transformations are parameterized by basis functions such as cosine and polynomials and constrained by prior information based on canonical brain anatomy [17]. Since Dixon AC and UTE AC data are derived from the same nonattenuated PET data, registration parameters were derived for the Dixon AC data, and the same registration parameters applied to both Dixon AC and UTE AC PET data to avoid any possible differences in registration for the two MR AC techniques.

Following registration, data were “count”-normalized. For data to be assessed in terms of activity concentration, CT AC PET data were rescaled to account for the radioactive decay between acquisition of the CT AC and MR AC data. To produce data in terms of SUV_r, a grey matter cerebellum mask was manually delineated on a high-quality T1 MRI scan in the same anatomical space as the coregistered PET data. Using this mask, PET data could be defined in terms of SUV_r referenced to the cerebellar grey matter using Matlab R2012a (Mathworks Inc., Natick, MA). Since the data were normalized to the cerebellum there was no requirement to account for the time of scan to count-normalize the SUV_r PET data.

Data analysis

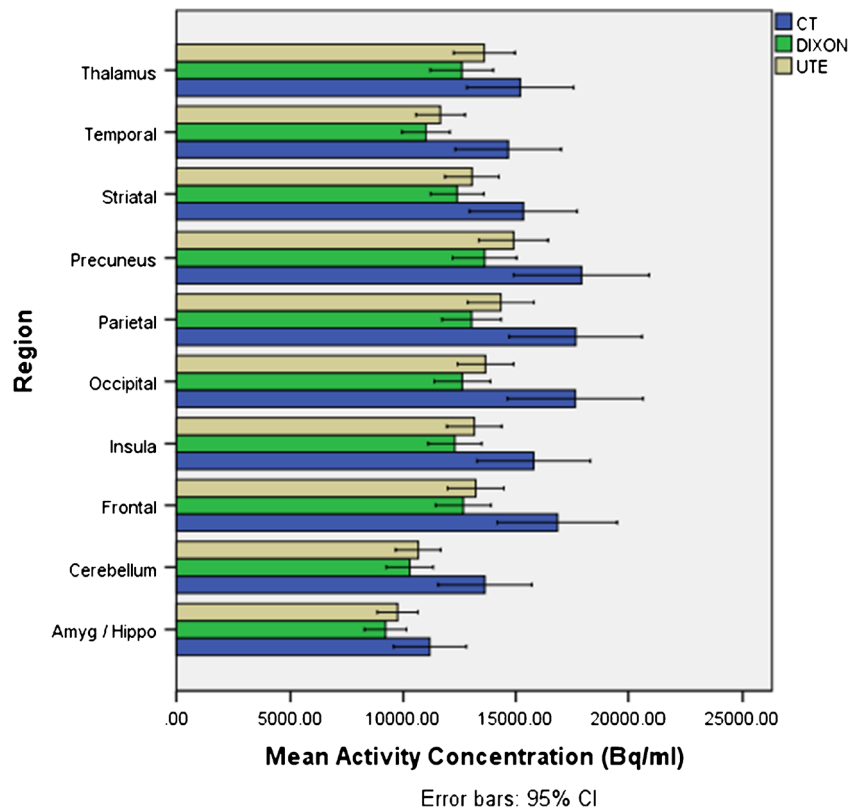
Using the MarsBaR toolbox for SPM [18], VOI analysis was performed on activity concentration and SUV_r data for ten regions commonly assessed in neurological PET: the amygdala/hippocampus, cerebellum, frontal lobes, insula, occipital lobes, parietal lobes, precuneus, striata, temporal lobes and thalamus. Differences between CT AC and Dixon AC, and CT AC and UTE AC methodologies were assessed in absolute and percentage terms with the significance of these differences determined using Student's paired *t* test. The significance of the changes seen with UTE AC compared with those seen with Dixon AC was also assessed using Student's paired *t* test. To examine relationships and biases between the ‘gold standard’ CT AC and MR AC methodologies, correlation and Bland-Altman analysis was performed. The statistical software used was IBM SPSS Version20. All tests were two-tailed with statistical significance determined as $P < 0.05$.

Voxel-based analysis to assess differences between CT AC and Dixon AC, and CT AC and UTE AC PET data was performed within SPM8 using a paired *t*-test methodology. All results were assessed at an uncorrected significance level of $P < 0.001$.

Results

VOI analysis in the ten selected regions showed that both Dixon AC and UTE AC significantly underestimated the activity concentrations in comparison with those derived using CT AC (Fig. 1, Table 2). Correlation and Bland-

Fig. 1 Mean regional activity concentrations derived using CT AC, Dixon AC and UTE AC. Error bars represent the 95 % confidence intervals on the means



Altman analysis confirmed this underestimation for most, but not all studies, with differences increasing with increasing activity concentration in the region. Example data showing this relationship are given in Fig. 2a for the frontal lobe, although all other regions showed similar associations. In terms of percentage difference, the average regional reduction in uptake ranged from a maximum of 21 % in the occipital lobes to a minimum of 11 % in the thalamus with Dixon AC, and 17 % in the cerebellum to 4 % in the thalamus with UTE AC. On a regional

basis, the use of UTE AC led to a significant reduction in the level of underestimation found with Dixon AC in all areas except the striata and cerebellum. The patterns of underestimation with MR AC compared to those with CT AC were reinforced in the voxel-based analysis (Fig. 3), with substantial and statistically significant underestimation of activity concentrations seen in the cortical and cerebellar regions with Dixon AC. The extent and significance of these differences were mostly reduced when UTE AC was applied.

Table 2 Differences in regional activity concentration between MR AC and CT AC PET data presented as means ± standard errors of all 25 subjects. The significance of these differences as determined using the

two-tailed Student's *t* test are also given together with the significance of the differences between Dixon AC and UTE AC

Region	Dixon AC		UTE AC		Dixon–UTE AC difference
	Difference (%)	<i>P</i> value	Difference (%)	<i>P</i> value	<i>P</i> value
Amygdala/hippocampus	-13.05±3.95	0.003	-8.69±3.23	0.013	0.017
Cerebellum	-19.80±3.84	0.001	-17.29±3.77	0.001	0.084
Frontal	-18.86±4.20	0.001	-15.66±4.09	0.001	0.001
Insula	-15.98±4.43	0.001	-10.73±4.19	0.017	0.001
Occipital	-21.30±4.57	0.001	-15.17±4.66	0.003	0.001
Parietal	-19.68±4.42	0.001	-12.16±4.58	0.014	0.001
Precuneus	-17.18±4.65	0.001	-9.90±4.67	0.044	0.001
Striatal	-12.54±4.74	0.014	-9.24±4.34	0.043	0.090
Temporal	-19.16±3.98	0.001	-15.18±3.69	0.001	0.001
Thalamus	-10.74±4.82	0.035	-4.32±4.35	0.331	0.001

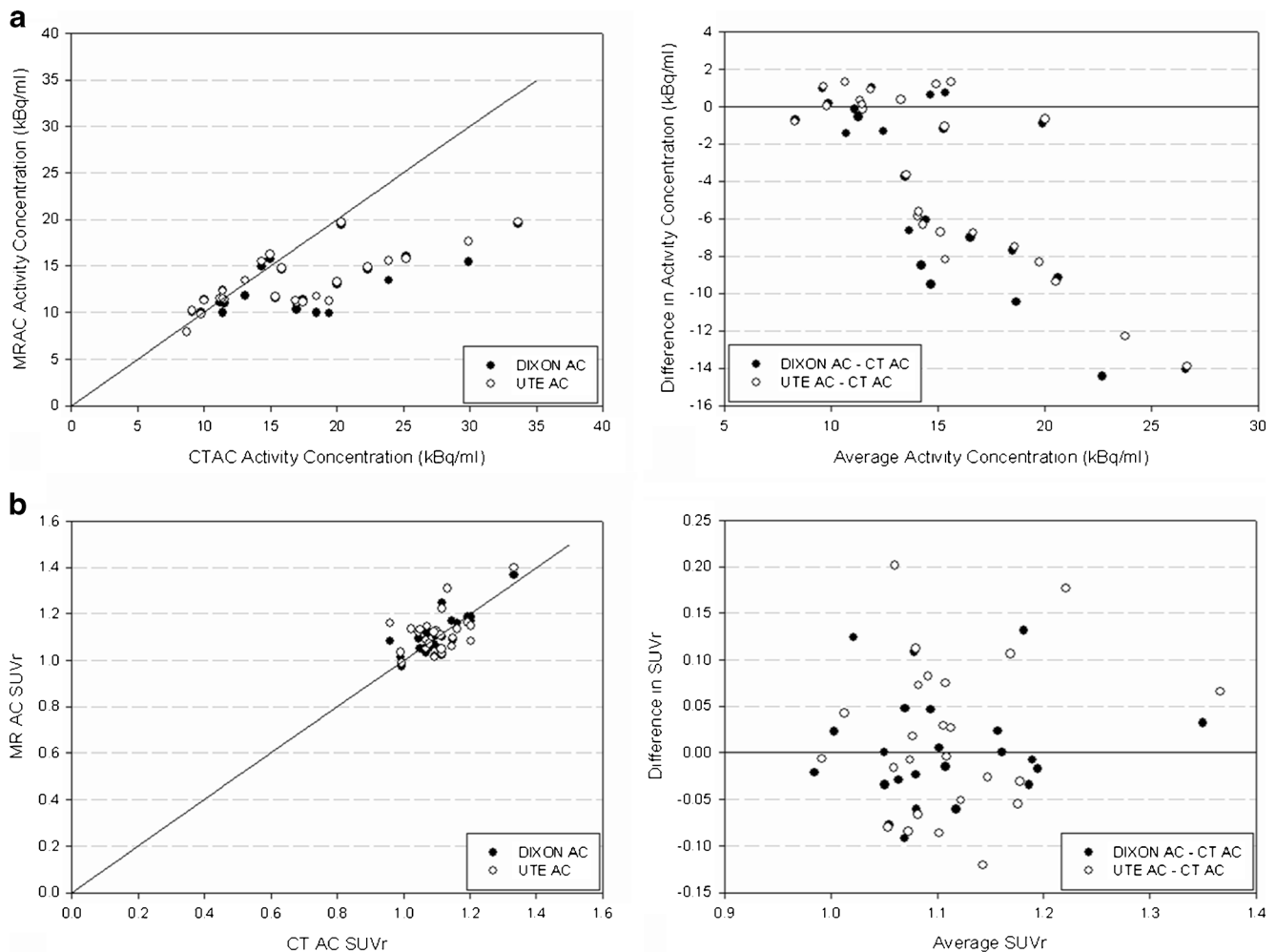


Fig. 2 Correlation and Bland-Altman analyses showing the relationships in the frontal lobe between CT and MR AC techniques with data represented as **a** activity concentrations and **b** SUVr

VOI results using SUVr are summarized in Fig. 4 and Table 3, with example correlation and Bland-Altman analysis for the frontal lobe shown in Fig. 2b. Both Dixon AC and UTE AC overestimated SUVr compared to CT AC in all subcortical areas in addition to the insula and precuneus cortical areas. However, the overestimation was not significant in the precuneus using Dixon AC. In the remaining cortical areas, underestimation was seen with Dixon AC, although it was only statistically significant in the occipital lobes. Overestimation was apparent with UTE AC – significantly so in the parietal and temporal lobes. In cerebellar areas, both MR AC techniques led to a small but statistically significant underestimation of uptake when compared to that derived using CT AC. Correlation analysis supported these findings, with Bland-Altman plots showing no underlying bias. Statistically significant differences in uptake determined using the two MR AC techniques were found in all regions with the exception of the cerebellum, frontal lobes and striata.

This mixed picture is generally supported in Figs. 5 and 6 which show highly significant areas of underestimation and

overestimation. Where there was underestimation with Dixon AC compared to CT AC (Fig. 5a), these areas of underestimation were limited to the most lateral elements of cortical regions. The right side of the brain also appeared to be more affected than the left. Most of these areas of underestimation were not seen with UTE AC (Fig. 5b), with only small differences seen in the frontal, temporal and cerebellar regions. Again there appeared to be some features indicating lateralization in these differences. In relation to overestimation of SUVr with MR AC compared to CT AC (Fig. 6), UTE AC showed more extensive and more significant areas of overestimation than those seen with Dixon AC. No features indicating lateralization were discernible in this comparison.

Discussion

The inaccuracy of attenuation correction in PET/MR due to the difficulty in defining bone tissue is of concern, particularly in the brain, which is surrounded by bone and where

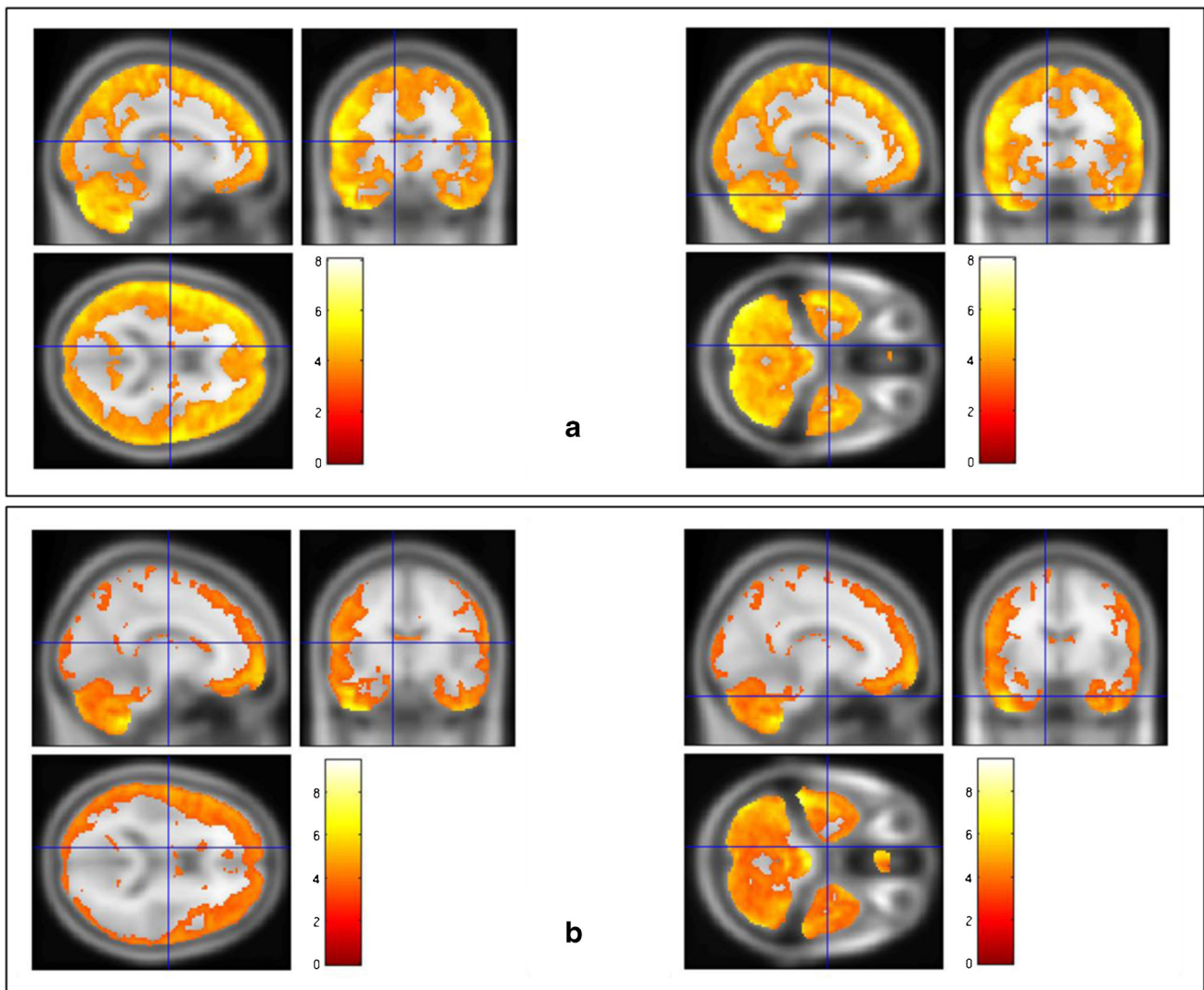
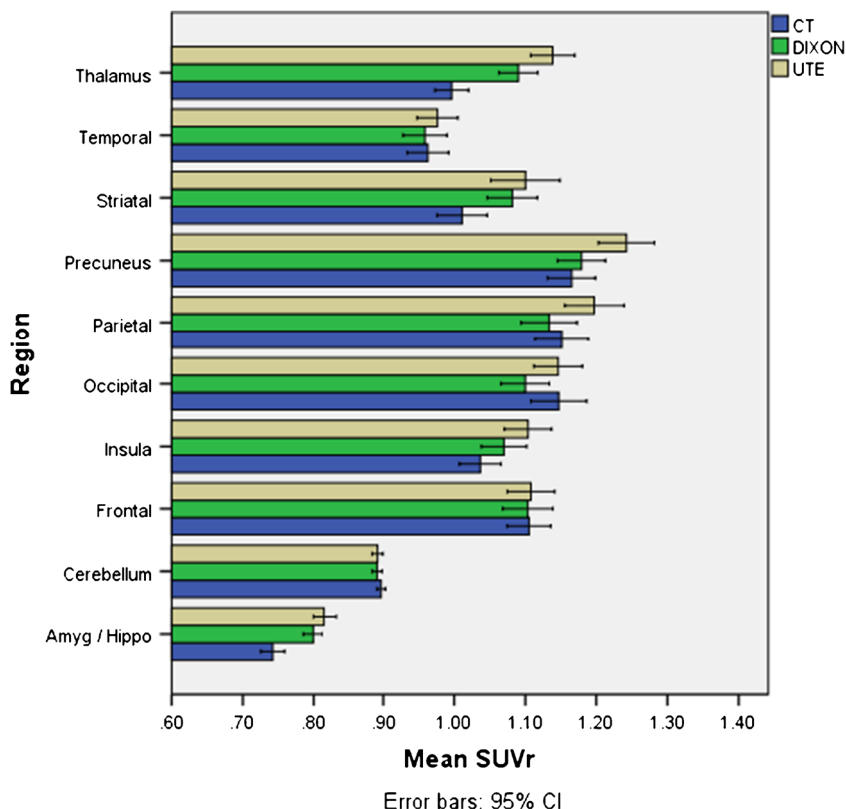


Fig. 3 Paired comparisons of activity concentrations derived from CT AC PET data and **a** Dixon AC PET data and **b** UTE AC PET data. The images show areas of underestimation with MR AC compared to CT AC at a significance level of $P < 0.001$ uncorrected

quantitative assessment of PET data may be essential. The findings of this study comparing clinical patient data from a simultaneous PET/MR scanner to that from PET/CT, highlight the extent of the issue using currently available technology. Our findings suggest that the use of standard Dixon AC methodologies used as a default in some simultaneous PET/MR scanners, can lead to underestimation of cortical activity concentrations as high as 21 %, with subcortical underestimation around 10 – 15 %. Voxel-based assessment of these differences showed the problem to be extensive in the grey matter, which makes accurate quantitative assessment of tracers such as FDG problematic. Furthermore, Bland-Altman analysis of regional data revealed an underlying trend in this underestimation with increasing differences between methods with increasing regional activity concentration, and even overestimation using Dixon techniques in some instances (Fig. 2a).

These findings are not unexpected. As activity concentration in an area increases, disparities in the attenuation maps will, through the multiplicative nature of AC, lead to increasing differences in PET uptake. Overestimation of uptake using Dixon AC in place of CT AC is also possible in some instances because of variability in anatomy and the segmentation process. Of course, the Dixon method was never recommended for brain work, which is why sequence-derived solutions such as that based on UTE imaging have been put forward as alternatives. However, our findings show that although the use of UTE AC led to significant improvements in the accuracy of PET uptake measurement (with reference to our gold standard) by reducing the severity and extent of areas of underestimation throughout the brain, underestimation of PET activity concentrations was still as high as 15 % in cortical areas reducing to around 4 % in areas such as the thalamus. Inaccuracy was most challenging, however, in the

Fig. 4 Mean regional SUVr derived using CT AC, Dixon AC and UTE AC. Error bars represent the 95 % confidence intervals on the means



cerebellum where the sinuses and bony areas around the sinuses can be difficult for both Dixon and UTE methodologies [19]. As with the Dixon method, there appeared to be variability and bias in this underestimation, and overestimation in a small number of cases.

Areas of underestimation are not unexpected using MR AC methods. Using Dixon AC, the lack of bone in attenuation maps (Fig. 7) will affect all PET lines of response passing through the skull. However, the greatest effects occur in or close to areas where there is a high density of bone tissue, because at oblique angles a greater proportion of the PET

raysums (integrals) will pass through bone [20]. The issue was improved with UTE AC; although, as can be seen in a typical UTE-based attenuation map, current segmentation of bone is basic with limited spatial resolution and imperfect segmentation (Fig. 7d). Particular problems for both techniques occurred in the inferior part of the brain, particularly around the cerebellum and inferior temporal lobe regions such as the temporal pole. In such regions, there can be difficulty in differentiating soft tissue from air (Dixon AC) and bone from soft tissue from air (UTE AC) in the sinuses, as is demonstrated in Fig. 8. The bones in this area such as the temporal bone,

Table 3 Differences in regional SUVr between MR AC and CT AC PET data presented as the means ± standard errors of all 25 subjects. The significance of these differences as determined using the two tailed Student's *t* test are also given together with the significance of the differences between Dixon AC and UTE AC

Region	Dixon AC		UTE AC		Dixon–UTE AC difference
	Difference (%)	<i>P</i> value	Difference (%)	<i>P</i> value	<i>P</i> value
Amyg / Hippo	7.92±1.18	0.001	10.22±1.11	0.001	0.004
Cerebellum	−0.82±0.25	0.003	−0.77±0.26	0.007	0.868
Frontal	−0.05±1.03	0.963	0.43±1.13	0.707	0.519
Insula	3.31±0.93	0.002	6.47±0.98	0.017	0.001
Occipital	−3.78±1.47	0.017	0.30±1.59	0.854	0.001
Parietal	−1.42±1.33	0.297	4.21±1.42	0.007	0.001
Precuneus	1.46±1.32	0.281	6.93±1.44	0.044	0.001
Striatal	7.33±1.12	0.001	8.25±1.49	0.043	0.474
Temporal	−0.17±0.61	0.782	1.50±0.66	0.001	0.001
Thalamus	9.57±1.05	0.001	14.27±0.94	0.001	0.001

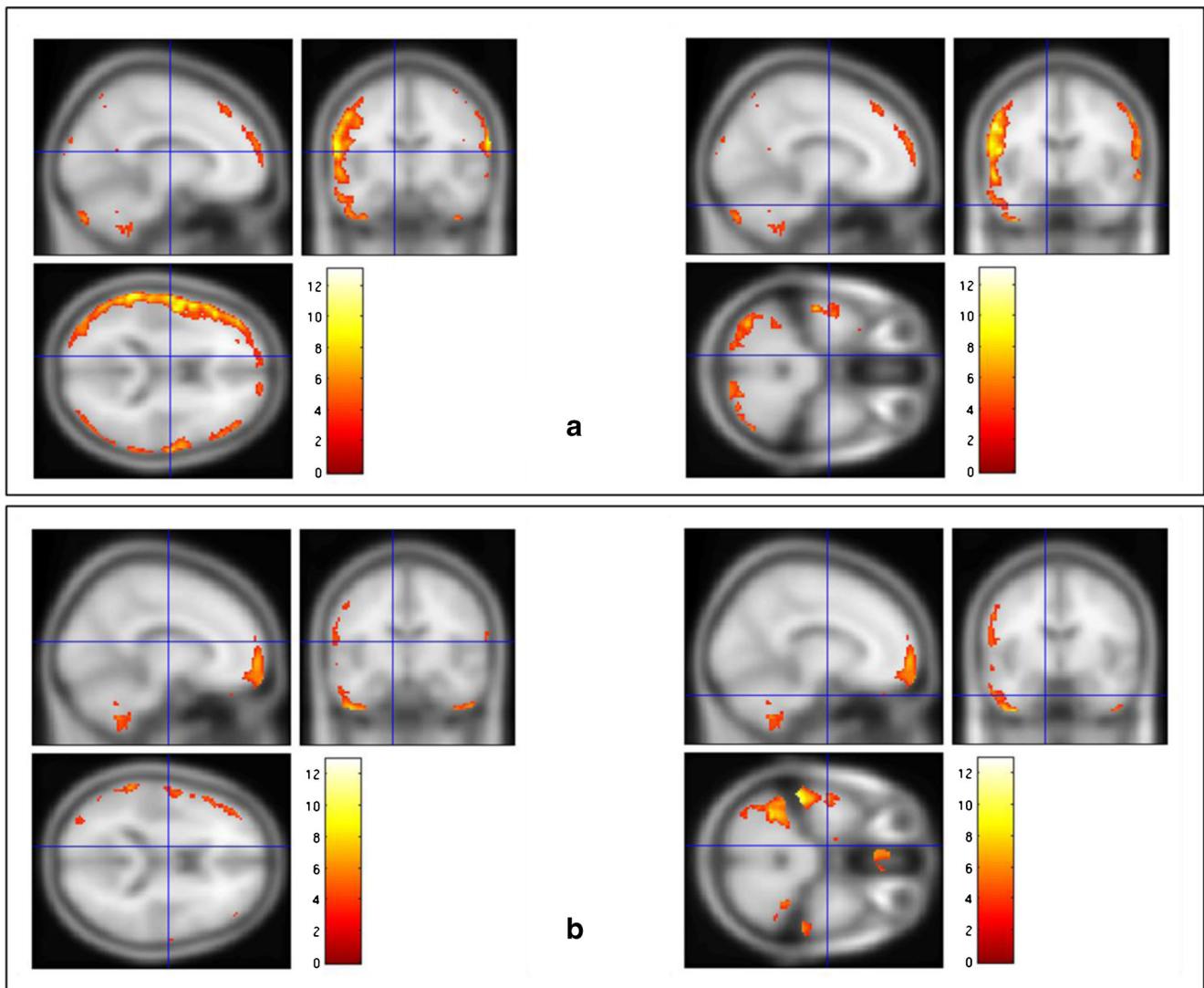


Fig. 5 Paired comparisons of SUVr derived from CT AC PET data and **a** Dixon AC PET data and **b** UTE AC PET data. The images show areas of underestimation with MR AC compared to CT AC at a significance level of $P < 0.001$ uncorrected

and wings of the sphenoid are of relatively low density, which results in the MR signals being difficult to accurately detect and segment, even with UTE sequences. This has the potential to produce areas where PET uptake is underestimated if bone/soft tissue is classified as air and overestimated if air is classified as bone/soft tissue.

Comparing our results with those of previous studies there are areas of both agreement and apparent disagreement. Regarding the underestimation, our results with Dixon AC generally match the findings of Samarin et al. [13] and Keereman et al. [15], both in the areas and magnitude of underestimation. Keereman et al. report areas of underestimation of up to 14 %, and Samarin et al. report underestimation of around 14–16 % in areas close to bone, which compares well with our findings of up to 20 % in the same area. Similarly, the underestimation of the PET signal in our UTE AC data is in good general agreement with the results reported by Catana et al. [21],

Keereman et al. [15] and Berker et al. [19] again in terms of the areas and magnitude of changes. Maximum areas of underestimation near bone were reported as 20–40 % by Keereman et al. and around 20 % by Berker et al. Our results suggest a maximum underestimation of 15 %.

However, there appears to be disagreement in the published data for both Dixon AC and UTE AC which, contrary to our results, also suggest areas of overestimation, most frequently around the sinuses, but also in other areas [15, 19, 21]. Why there would be areas of overestimation in the middle of the brain around and superior to the ventricles is difficult to explain since the absence of bone tissue for the Dixon AC, or incompleteness of bone tissue for UTE AC would lead to underestimation of uptake for all lines of response through the skull, which would be more significant in areas close to the skull itself. Areas of overestimation around the sinuses are easier to understand as described above, although these were

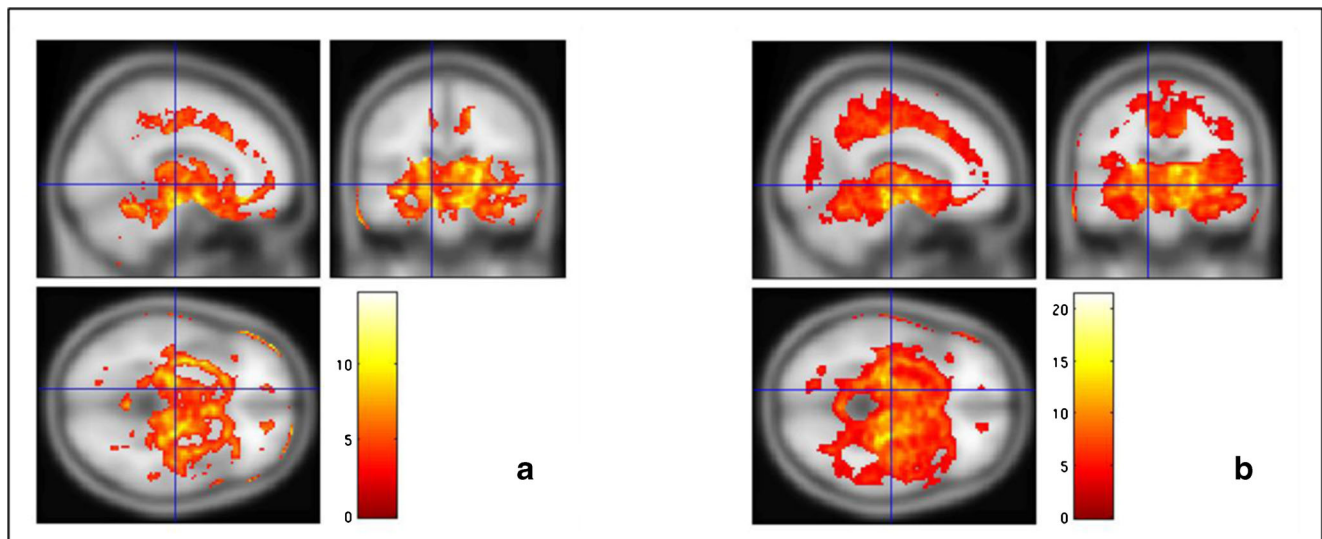


Fig. 6 Paired comparisons of SUVR derived from CT AC PET data and **a** Dixon AC PET data and **b** UTE AC PET data. The images show areas of overestimation with MR AC compared to CT AC at a significance level of $P < 0.001$ uncorrected

not apparent in our group analysis. Why there appears to be discordance between our and published results, particularly with UTE AC, can be partly attributed to methodological differences in acquisition technique, segmentation, and indeed the attenuation coefficients assigned to the different tissue types. For the first two factors, this can be seen with a wide range in UTE AC map quality in this study and in the

literature. However, apparent differences between the MR AC techniques can also be ascribed to the methods of analysis used in this and the other studies. In our regional analysis we defined our results based on volumes that could be quite substantial in extent. This approach was chosen since analysis of PET data is frequently performed using such regions, although it may of course dilute areas of overestimation found

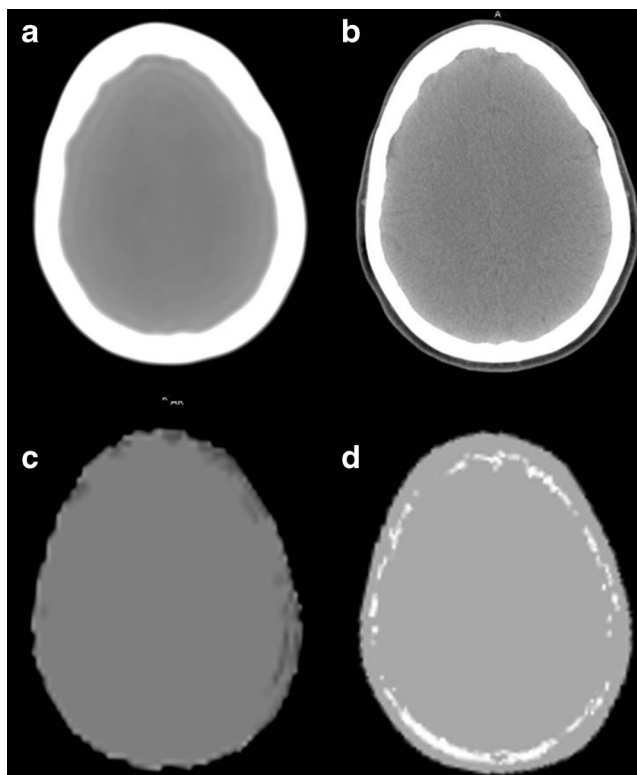


Fig. 7 Superior slices of a brain showing **a** CT AC data, **b** CT with a standard reconstruction filter, **c** Dixon AC data and **d** UTE AC data

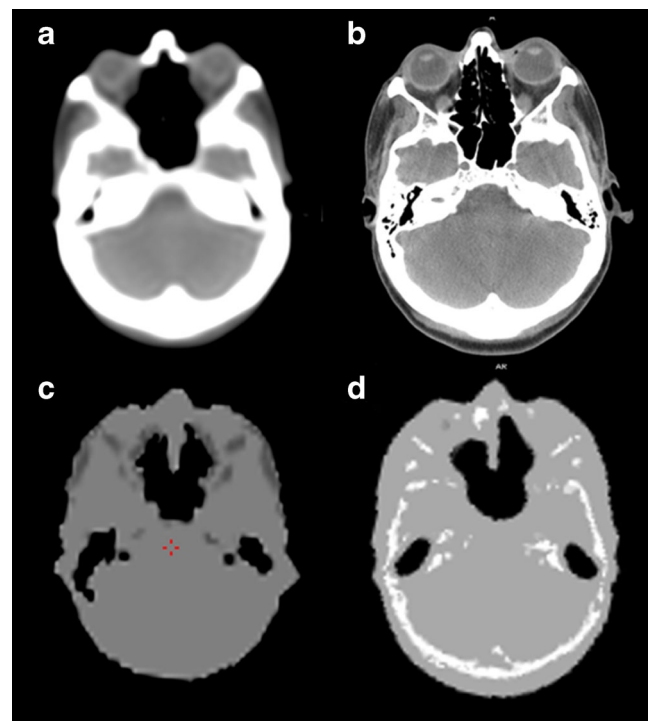


Fig. 8 Inferior slices of a brain showing temporal bones represented using **a** CT AC data, **b** CT with a standard reconstruction filter, **c** Dixon AC data and **d** UTE AC data

in the literature. Furthermore, while others have performed analyses in single subjects or small groups, in our group-wise analysis of 25 patients we found that no areas of overestimation predominated in the group as a whole. Of course, on an individual subject basis (Fig. 2), in a small number of areas PET uptake was overestimated. In our voxel-based analysis, although areas of overestimation may exist on an individual basis, the statistical analysis over our groups of data showed no areas of significant overestimation. Because of the variable quality of MR AC maps within and between subjects, this lack of areas of significant overestimation could again be attributed to an increased variance caused by the differing levels of regional success in MR AC map creation process over the whole group.

The errors in regional activity concentrations translated through to the data represented as SUVr with a grey matter cerebellum reference volume. Instead of accounting for the general errors in MR AC, the inaccuracy in cerebellar activity concentrations led to a mix of areas of underestimation and overestimation of SUVr with no underlying bias in the differences. In percentage terms, the regional difference between CT AC and MR AC PET data appears to be less than the difference in activity concentration data, and at the voxel level the extent of the difference also decreased. However, at the statistical level, SPM highlighted a higher level of cortical underestimation in both the Dixon AC and UTE AC comparisons, with the additional confounder of extremely significant areas of overestimation in subcortical areas that were absent in the activity concentration data. There are some apparent inconsistencies between regional and voxel-based methodologies such as significant cortical overestimation of SUVr using a regional approach which are seen as highly significant areas of underestimation in voxel-based analysis. However, this can easily be explained by the very focused and lateralized areas of underestimation (Fig. 4b) being diluted when represented by large bilateral regions.

The right–left asymmetry in SUVr and activity concentration data was unexpected. Using the MarsBaR toolbox, right-sided and left-sided regional data were derived but subsequently conjugated for our analysis. In right-sided and left-sided regions in the midfrontal and midoccipital lobes where lateralization in voxel-wise SUVr differences seemed greatest, significant regional differences were also seen. Indeed in the midoccipital lobe, significant differences (right more than left) were also seen in the Dixon AC and UTE AC activity concentration data. Why these left-to-right differences occurred is not known, but the differences may have been due to local field inhomogeneities producing missegmentation in the MR-derived AC maps. In its simplest form, tissue segmentation is based on simple thresholding of images at multiple levels of voxel intensity. More sophisticated techniques use clustering algorithms in conjunction with probabilistic models based both on information from histograms of voxel intensity and on neuroanatomical information. All of these techniques,

however, are sensitive to a lesser or greater extent to partial volume effects, distortion and uniformity as well as signal-to-noise and contrast-to-noise ratios in the images so that any subsequent measurements of tissue volume would necessarily include variability due to variations in both image quality and anatomy, but these effects can be partly corrected for using postprocessing techniques. Since the Siemens PET MR AC correction tools are not available to users it is impossible to ascertain the effect on the PET data of using uncorrected or corrected bias AC maps. However, we were able to establish the presence of a right-to-left difference in field homogeneity in many patients (Fig. 9) using N3 software tools [22] which resulted in an average difference of 2,070 bone-assigned voxels between the corrected and uncorrected UTE AC acquisitions. This highlights the fundamental difficulties in using the MR signal to provide AC for PET data, and in order to use data reconstructed using this method for semiquantitative analysis it is essential to build scanner-specific normal databases for comparisons.

To put these effects into context it is helpful to see how they translate into clinical interpretations of data. Figure 10 shows three global count-normalized 3-D SSP surface-rendered representations [23] of the brain of a patient with epilepsy demonstrating mild bilateral temporal hypometabolism, with three images showing PET data attenuation-corrected using CT-, Dixon- and UTE-based attenuation maps. Using CT AC, the patient is seen to have mild areas of hypometabolism in the poles and inferior aspects of both temporal lobes, with the remaining territories showing relatively good, even metabolism. When Dixon AC is applied, a global reduction in metabolism is seen, with lateral, inferior and superior areas affected more than medial aspects. Because of this effect, the hypometabolism in the temporal lobes is more exaggerated than that seen when CT AC is applied. Using UTE AC, some

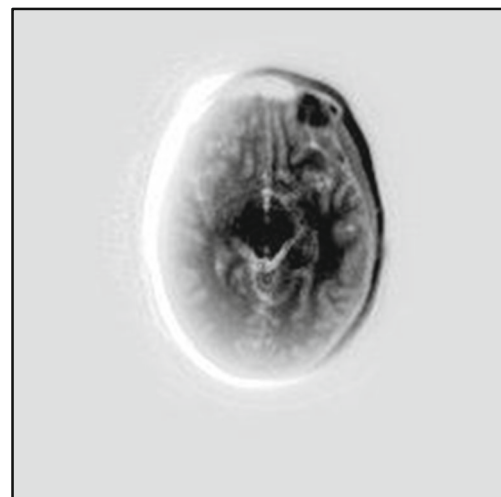
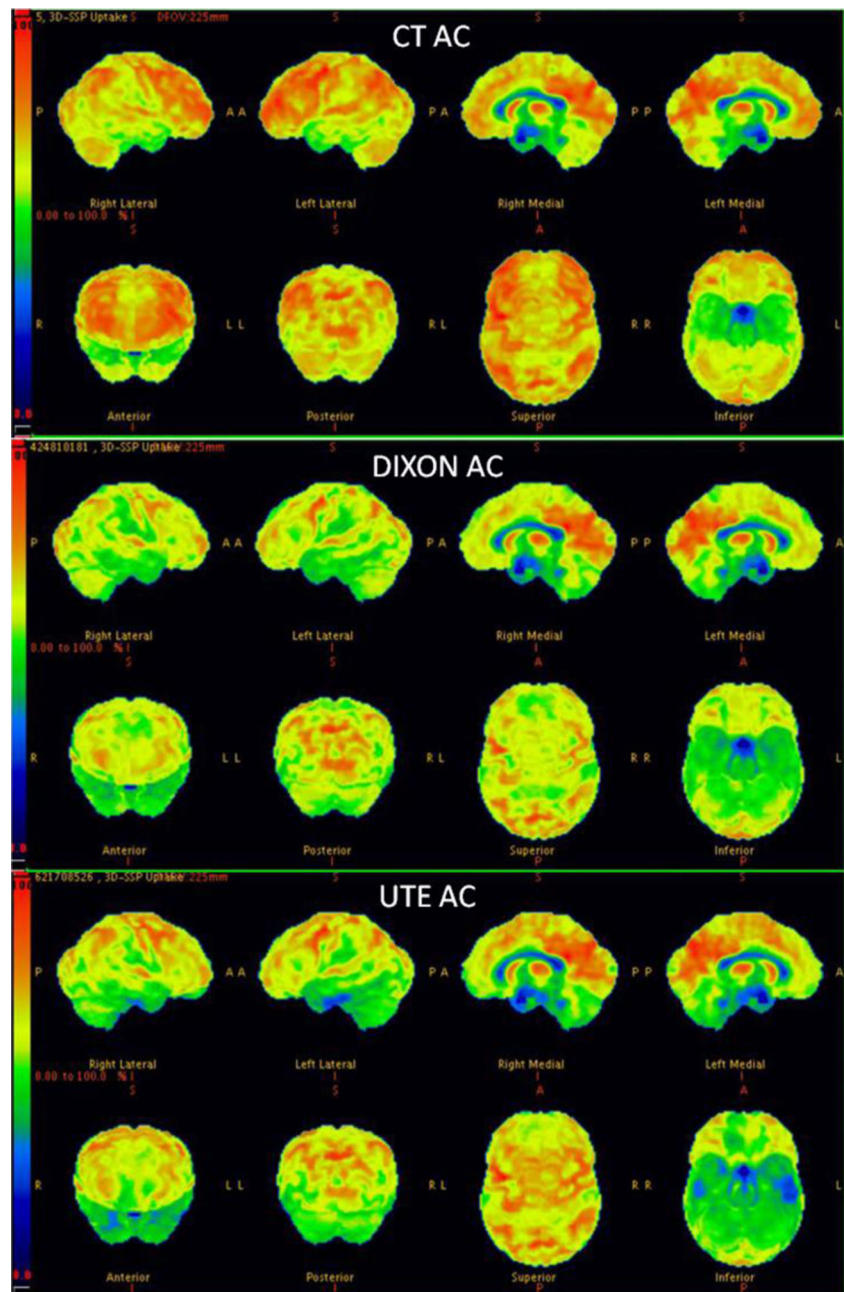


Fig. 9 An example of field inhomogeneity in the first echo of the UTE sequence as determined using N3 software. The data represented are uncorrected data minus corrected data

Fig. 10 3-D SSP surface-rendering maps of the brain of a patient with epilepsy using PET data attenuation-corrected using CT, Dixon- and UTE-based attenuation maps



of the loss in global metabolism is recovered from that seen using Dixon AC, but the inferior areas of the brain nearer the sinuses and lower skull structures show further reduced areas of metabolism compared to the pattern seen using CT AC, particularly in the poles and inferior aspects of both temporal lobes. The global reduction in calculated activity concentrations with Dixon AC compared to CT AC compares well with our group findings, as does the partial recovery of attenuation losses and bone/sinus segmentation difficulties when UTE AC is used.

As mentioned above, our study was performed using ‘out-of-the-box’ methods provided by the scanner manufacturers,

and there were inevitably some differences between ours and previously described techniques. Although full details of the techniques we used are not completely within the public domain, we can speculate as to where the differences may lie, namely the acquisition parameters, segmentation algorithms, and the PET attenuation values used. For Dixon-based attenuation maps there are currently two scanner-specific methodologies [12, 24] with the Martinez-Möller method [12] used in our simultaneous PET/MR device. Similar to all MRI devices there are small differences between the MR acquisition processes across devices/manufacturers, but the key difference with these techniques is the segmentation algorithm used. On

our scanner, a four-tissue segmentation (air, fat, soft tissue, and lungs) is used, while the alternative combines the fat and soft tissue segmentation into one soft tissue class. Although the results from these two techniques are similar [24], the segmentation into more rather than fewer tissue classes is deemed to lead to more accurate PET uptake values [24, 25], suggesting that our results represent the best currently achievable accuracy with Dixon-based methods.

The differences between UTE methodologies currently available are greater than those seen with Dixon-based techniques, reflecting the fact that these methods are currently under continuing development and optimization. One clear difference between the technique used in our methods and those used in previously published studies is the acquisition parameters used, with the scan duration in our work much shorter than that used in other studies [15, 21]. The driver for a shorter scan duration is the demand for other MR sequences to be run whilst the PET scan is running; however, this has come at the cost of poorer image quality. This choice is more likely to lead to poorer segmentation of data, and in turn poorer quantitative accuracy [26]. It is expected that continuing optimization and future developments will improve the performance of UTE AC, although the challenges of accurate capture and segmentation of tissue bone and air, particularly around the sinuses will remain. Additionally, the PET attenuation coefficient values used for both MR AC methods may also have led to differences between our and previously published results. There is currently little consensus as to the appropriate values to use [14], although the effects of using different values are understood [26].

There were some potential limitations in our study. The primary limitation was that PET data derived using CT AC and MR AC were acquired sequentially on different scanners. To overcome any bias in the PET data relating to time after injection, we randomly streamed patients into PET/CT or PET/MR. Retrospectively, we found no significant difference in scan time between the groups. There were also small performance differences between the scanners involved, particularly in terms of spatial resolution and sensitivity. As much as possible the acquisition and processing protocols were matched to produce images of similar quality, although for sensitivity this is challenging given the fact that the brain almost fills the field of view on PET/CT, but only partially fills it on PET/MR. Nevertheless, even if there were residual differences caused by scan time or scanner performance, such differences would have led to a spatially invariant bias. Our data show differences that changed between brain regions, and our results showed the greatest differences between AC methods closest to bone, and the smallest differences in sub-cortical areas. This is better explained by the differences in AC maps than any by small performance differences in the reconstructed PET data.

Further technical limitations included the difference in slice thickness between CT AC and MR AC maps, and also the fixed linear attenuation coefficients used in MR AC maps. These issues are common to other studies in this area [19] and a workable solution would be difficult to find. The methodology for sequential scanning also led to the possibility of external stimuli before and between scans. However, the uptake environment was similar in the PET/CT and PET/MR suites, and scans were performed at a time after injection at which free FDG in the bloodstream would have been minimal and likely to have caused only small perturbations in the overall FDG signal. Furthermore, had any perturbations to existed, these would probably have become even less significant in the group analysis, and likely if anything to have increased the variance in the groups, and therefore to have decreased the probability of significant differences. To overcome the effects of possible differences in scanner performance, scan time, or tracer uptake between scans, it would have been useful to have had a method to compare the data from each scanner in the absence of any attenuation maps, i.e. using data without attenuation correction (non-AC data). However, the signal and also the noise/variance in non-AC data change dramatically on moving from the edge to the centre of the brain, which would make such statistical comparisons invalid for both VOI and SPM approaches.

Another possible limitation is that our subjects were patients clinically referred for a PET scan. Ethical considerations make scanning healthy control subjects to acquire a snapshot of current technology difficult to justify. Our patients were mostly young (younger than 40 years), and therefore had limited anatomical features/atrophy that could have confounded the results. However, almost all had areas of hypometabolism with 17 of the 22 abnormal patients demonstrating reduced uptake in the temporal lobes. The effect of these areas of hypometabolism would not therefore have been an issue outside this region. Furthermore, looking at the patterns throughout the brain, the results in neighbouring regions were not dissimilar to that in the temporal lobes, which suggests that the effect of hypometabolism in this region had a limited effect on the results.

Finally, we assumed that CT attenuation was the gold standard. Because of the challenges of converting the attenuation coefficients of a spectrum of low-energy photons from CT to the appropriate monoenergetic high-energy attenuation coefficient required for PET, the method is not without its errors [9, 27, 28], particularly since the CT scan was performed separately from the PET scan. However, since we took all possible steps to minimize misregistration between the PET and CT data, and because attenuation maps derived from CT and a 511 keV transmission source have been found to be effectively equivalent [29], we feel that CT AC can be considered a strong ‘gold standard’ comparator.

Overall, our findings strongly suggest that quantitative neurological PET/MR is not reliable with currently available

methods of MR AC. Representation in terms of activity concentrations showed substantial and significant areas of underestimation, with SUVr data referenced to the grey matter cerebellum showing a mixture of predominantly cortical underestimation and subcortical overestimation. Furthermore, with underestimation of activity concentrations in all areas of the brain, alternative reference regions would also be unreliable for the creation of SUVr data.

The results reported here offer a snapshot of the current limitations of MR AC for PET. However, the presence of a problem with available methodologies is well known [14], and there are continuing efforts within the community to produce improved techniques. This does not mean that neurological PET/MR is of no value. In neurooncology, the advantage of knowing where there is viable tumour by superimposing functional PET data onto MR anatomy is extremely valuable, with the visual assessment of data more than adequate for scan interpretation. Also, in neurodegenerative diseases, the presence of multimodality MR and PET information, even if the PET data are quantitatively compromised is still very powerful to understand the patient's condition better. The presence of PET/MR as a modality is very important for neurological imaging, and with the advent of new technologies will only improve further.

Conclusion

MR AC leads to a significant underestimation of activity concentration within the whole brain, but particularly in cortical grey matter and in the cerebellum. These effects limit the quantitative accuracy of neurological PET/MR represented either in terms of activity concentration or SUVr referenced to the commonly used grey matter cerebellum.

Acknowledgments This study was supported by the National Institute for Health Research, University College London Hospitals Biomedical Research Centre.

Conflicts of interest None.

References

- Catana C, Guimaraes AR, Rosen BR. PET and MR imaging: the odd couple or a match made in heaven? *J Nucl Med*. 2013;54:815–24.
- Fass L. Imaging and cancer: a review. *Mol Oncol*. 2008;2:115–52.
- Catana C, Benner T, van der Kouwe A, Byars L, Hamm M, Chonde DB, et al. MRI-assisted PET motion correction for neurologic studies in an integrated MR-PET scanner. *J Nucl Med*. 2011;52:154–61.
- Chun SY, Reese TG, Ouyang J, Guerin B, Catana C, Zhu X, et al. MRI-based nonrigid motion correction in simultaneous PET/MRI. *J Nucl Med*. 2012;53:1284–91.
- Rousset OG, Ma Y, Evans AC. Correction for partial volume effects in PET: principle and validation. *J Nucl Med*. 1998;39:904–11.
- Thomas BA, Erlandsson K, Modat M, Thurfjell L, Vandenberghe R, Ourselin S, et al. The importance of appropriate partial volume correction for PET quantification in Alzheimer's disease. *Eur J Nucl Med Mol Imaging*. 2011;38:1104–19.
- Vunckx K, Atré A, Baete K, Reilhac A, Deroose CM, Van Laere K, et al. Evaluation of three MRI-based anatomical priors for quantitative PET brain imaging. *IEEE Trans Med Imaging*. 2012;31:599–612.
- Yankeelov TE, Peterson TE, Abramson RG, Garcia-Izquierdo D, Arlinghaus LR, Li X, et al. Simultaneous PET-MRI in oncology: a solution looking for a problem? *Magn Reson Imaging*. 2012;30:1342–56.
- Kinahan PE, Townsend DW, Beyer T, Sashin D. Attenuation correction for a combined 3D PET/CT scanner. *Med Phys*. 1998;25:2046–53.
- Hofmann M, Pichler B, Schölkopf B, Beyer T. Towards quantitative PET/MRI: a review of MR-based attenuation correction techniques. *Eur J Nucl Med Mol Imaging*. 2009;36 Suppl 1:S93–S104.
- Coombs BD, Szumowski J, Coshov W. Two-point Dixon technique for water-fat signal decomposition with B0 inhomogeneity correction. *Magn Reson Med*. 1997;38:884–9.
- Martinez-Möller A, Souvatzoglou M, Delso G, Bundschuh RA, Chef'd'hotel C, Ziegler SI, et al. Tissue classification as a potential approach for attenuation correction in whole-body PET/MRI: evaluation with PET/CT data. *J Nucl Med*. 2009;50:520–6.
- Samarin A, Burger C, Wollenweber SD, Crook DW, Burger IA, Schmid DT, et al. PET/MR imaging of bone lesions – implications for PET quantification from imperfect attenuation correction. *Eur J Nucl Med Mol Imaging*. 2012;39:1154–60.
- Wagenknecht G, Kaiser H-J, Mottaghy FM, Herzog H. MRI for attenuation correction in PET: methods and challenges. *MAGMA*. 2013;26:99–113.
- Keereman V, Fierens Y, Broux T, De Deene Y, Lonneux M, Vandenberghe S. MRI-based attenuation correction for PET/MRI using ultrashort echo time sequences. *J Nucl Med*. 2010;51:812–8.
- Camus V, Payoux P, Barré L, Desgranges B, Voisin T, Tauber C, et al. Using PET with 18F-AV-45 (florbetapir) to quantify brain amyloid load in a clinical environment. *Eur J Nucl Med Mol Imaging*. 2012;39:621–31.
- Ashburner J, Friston KJ. Nonlinear spatial normalization using basis functions. *Hum Brain Mapp*. 1999;7:254–66.
- Brett M, Anton J-L, Valabregue R, Poline J-B. Region of interest analysis using the MarsBar toolbox for SPM 99. Sendai, Japan; 2002.
- Berker Y, Franke J, Salomon A, Palmowski M, Donker HCW, Temur Y, et al. MRI-based attenuation correction for hybrid PET/MRI systems: a 4-class tissue segmentation technique using a combined ultrashort-echo-time/Dixon MRI sequence. *J Nucl Med*. 2012;53:796–804.
- Andersen FL, Ladefoged CN, Beyer T, Keller SH, Hansen AE, Højgaard L, et al. Combined PET/MR imaging in neurology: MR-based attenuation correction implies a strong spatial bias when ignoring bone. *Neuroimage*. 2013;84C:206–16.
- Catana C, van der Kouwe A, Benner T, Michel CJ, Hamm M, Fenchel M, et al. Toward implementing an MRI-based PET attenuation-correction method for neurologic studies on the MR-PET brain prototype. *J Nucl Med*. 2010;51:1431–8.
- Sled JG, Zijdenbos AP, Evans AC. A nonparametric method for automatic correction of intensity nonuniformity in MRI data. *IEEE Trans Med Imaging*. 1998;17:87–97.
- Minoshima S, Frey KA, Koeppe RA, Foster NL, Kuhl DE. A diagnostic approach in Alzheimer's disease using three-dimensional stereotactic surface projections of fluorine-18-FDG PET. *J Nucl Med*. 1995;36:1238–48.
- Schulz V, Torres-Espallardo I, Renisch S, Hu Z, Ojha N, Börmert P, et al. Automatic, three-segment, MR-based attenuation correction for

- whole-body PET/MR data. *Eur J Nucl Med Mol Imaging*. 2011;38:138–52.
25. Marshall HR, Prato FS, Deans L, Théberge J, Thompson RT, Stodilka RZ. Variable lung density consideration in attenuation correction of whole-body PET/MRI. *J Nucl Med*. 2012;53:977–84.
 26. Schleyer PJ, Schaeffter T, Marsden PK. The effect of inaccurate bone attenuation coefficient and segmentation on reconstructed PET images. *Nucl Med Commun*. 2010;31:708–16.
 27. Nakamoto Y, Osman M, Cohade C, Marshall LT, Links JM, Kohlmyer S, et al. PET/CT: comparison of quantitative tracer uptake between germanium and CT transmission attenuation-corrected images. *J Nucl Med*. 2002;43:1137–43.
 28. Keat N, Hallett W, Howard J, Searle G. Assessment of quantitative PET image accuracy and uniformity using geometric and realistic brain phantoms. *J Nucl Med*. 2012;53 Suppl 1:2280.
 29. Burger C, Goerres G, Schoenes S, Buck A, Lonn AHR, Von Schulthess GK. PET attenuation coefficients from CT images: experimental evaluation of the transformation of CT into PET 511-keV attenuation coefficients. *Eur J Nucl Med Mol Imaging*. 2002;29:922–7.